Negative Local Permeability in $Bi_2Sr_2CaCu_2O_8$ Crystals

N. Morozov, E. Zeldov, D. Majer, and B. Khaykovich

Department of Condensed Matter Physics, The Weizmann Institute of Science, 76100 Rehovot, Israel

(Received 31 July 1995)

The local ac magnetic response in $Bi_2Sr_2CaCu_2O_8$ crystals was measured using a microscopic array of Hall sensors. The ac component of the local induction is found to attain negative values in contradiction with the standard models that predict a positive in-phase variation of the induction with the applied field. A model of ac response in the presence of a geometrical barrier is derived and is shown to describe well the measured behavior. The dissipation peak and the onset of higher harmonics at elevated temperatures are due to geometrical barrier and do not reflect a change in the bulk resistivity.

PACS numbers: 74.60.Ec, 74.60.Ge, 74.60.Jg, 74.72.Hs

Measurement of ac magnetic susceptibility is one of the most commonly used characterization tools for the study of high-temperature superconductors (HTSC). A wide range of superconducting properties is being inferred from ac studies which include irreversibility line, resistivity, critical current, pinning mechanism, nonlinear response, vortex-lattice melting, etc. [1–10]. The standard approach to the description of the ac response is based on the perception that the ac magnetic field perturbation inside the superconductor penetrates through the edges of the sample and decays monotonically towards the center with some characteristic length scale. For given amplitude and frequency of the applied ac field and sample geometry, the ac penetration depth is usually assumed to be determined by either the linear resistivity, the nonlinear resistivity, or the critical current [11–19]. The in-phase local permeability $\mu' = 1 + 4\pi\chi'$, where χ' is the local susceptibility, measures the shielding response which is expected to be *positive* everywhere across the sample—high close to the sample edges (poor shielding) and low in the center (good shielding). The out-of-phase μ'' or χ'' describe the energy dissipation in the sample. This dissipation is expected to have a sharp maximum as a function of temperature or applied dc field when the sample resistivity or critical current are such that the ac penetration depth is comparable to the sample dimensions [14–19]. In this paper we show experimentally that in striking contrast to the above description in clean $Bi_2Sr_2CaCu_2O_8$ (BSCCO) crystals at elevated temperatures the local μ' obtains *negative* values and the peak in χ'' is *unrelated* to the sample resistivity and critical current. This unique behavior is shown to be the result of the geometrical barrier [20–25] that is not taken into account in the prevailing models.

A high quality rectangular BSCCO crystal ($T_c = 90$ K) of $240 \times 300 \times 40$ μm^3 was attached directly to the surface of an array of eleven 10×10 μm^2 Hall sensors fabricated photolithographically using GaAs/AlGaAs heterostructure [26]. A dc magnetic field was applied using a large bore superconducting magnet operated in constant current mode, and the ac field was generated by a small copper coil with $H_{dc} \parallel H_{ac} \parallel c$ axis of the crystal. The ac component of the perpendicular local induction B_{ac} at the sample surface was measured by the sensors using lock-in techniques as a function of H_{dc} and temperature. H_{dc} and H_{ac} were measured directly by additional Hall sensors residing outside the sample.

We consider a sample in a form of a long rectangular strip of thickness d and width $2W$ along x in perpendicular applied field $H_a \parallel z$. In a platelet sample in the perpendicular field, the vortex potential has a minimum value in the center of the sample and a significant potential barrier close to the edges [20–25]. This geometrical barrier (GB) is absent in samples with elliptical or tapered cross sections [27]. In platelet crystals in the absence of bulk pinning, at H_a larger than the penetration field H_p, the vortices penetrate irreversibly over the GB and focus in the center of the sample due to the Lorentz force of the Meissner current. The resulting vortex droplet has a dome-shaped profile of the local field $B_z(x)$ as shown in Fig. 1. The field profile is described by two parameters, the width of the droplet $2b$ and the width of the narrow edge region $W - e$ where vortices cut through the sample rims, resulting in [20]

$$B_z(x) = \frac{2H_{c1}}{\pi} \ln \frac{\sqrt{|e^2 - x^2|(W^2 - b^2)} + \sqrt{|b^2 - x^2|(W^2 - e^2)}}{\sqrt{(e^2 - b^2)|W^2 - x^2|}} \tag{1}$$

at $|x| < b$ and $|x| > e$, whereas $B_z(x) = 0$ in the vortex-free region at $b \le |x| \le e$. The corresponding applied field is

$$H_a = \frac{2H_{c1}}{\pi} \ln \frac{\sqrt{W^2 - b^2} + \sqrt{W^2 - e^2}}{\sqrt{e^2 - b^2}}, \tag{2}$$

with resulting global magnetization per unit volume of

$$M = -\frac{H_{c1}}{4\pi W d} \sqrt{(W^2 - b^2)(W^2 - e^2)}. \tag{3}$$

On increasing dc field $H_{dc} \ge H_p$ the parameter $e \simeq W - d/2$, and the droplet expands with the field according to

 0031-9007/96/76(1)/138(4)$06.00

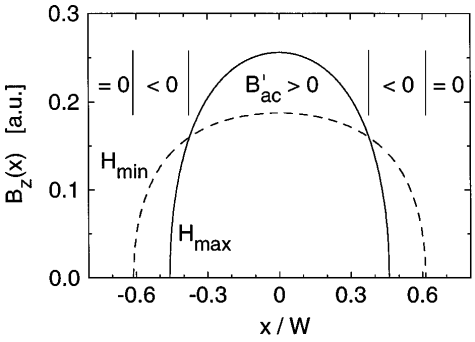

FIG. 1. The theoretical dome-shaped field profile $B_z(x)$ of the vortex droplet in the center of the sample at extreme values of the applied field.

Eq. (2) as additional vortices penetrate. On decreasing field, however, the droplet is extended to the edges and its half-width $b \simeq W - d/2$ is constant as vortices leave the sample. As a result, the GB gives rise to a hysteretic dc magnetization loop as shown in Fig. 2. The corresponding experimental local magnetization loop $B_{\rm dc} - H_{\rm dc}$ in BSCCO at $T = 80$ K, as measured by the Hall sensors in the central region of the crystal, is shown in the inset.

We now derive the ac response in the presence of GB. Let us consider application of a small ac field of amplitude $H_{\rm ac}$ at some given value of dc field on the ascending branch such as point 1 in Fig. 2. The number of vortices in the droplet is determined by the peak value of the field $H_{\rm max} = H_{\rm dc} + H_{\rm ac}$. As the instantaneous applied ac field decreases, the central vortices cannot leave the sample since they are trapped by the Meissner current that continues to circulate in the same direction. The magnitude of the current decreases, and the droplet broadens out, maintaining the total number of trapped vortices constant (Fig. 1). The parameters b and e are determined by the instantaneous H_a through Eq. (2) and by the requirement of a constant trapped flux $\Phi = \int_{-b}^{b} B_z(x)dx = \text{const} \times (H_{\rm max})$. The resulting trajectory of the global ac magnetization is shown in Fig. 2 by the dashed curve. Locally, however, a unique situation occurs.

Figure 1 shows the field distribution in the central region at the extreme values of the applied field $H_{\rm max}$ and $H_{\rm min} = H_{\rm dc} - H_{\rm ac}$. We define the local permeability $\mu(x) = \mu' - i\mu'' = (B'_{\rm ac} - iB''_{\rm ac})/H_{\rm ac}$, where $B'_{\rm ac}(x)$ and $B''_{\rm ac}(x)$ are the amplitudes of the in-phase and out-of-phase ac components of the local field $B_z(x)$. In the sample center, $B_z(x)$ increases with H_a, and hence the local permeability is positive. However, close to the droplet edges, $B_z(x)$ *decreases* with increasing instantaneous H_a, and hence $B'_{\rm ac}(x)$ is in antiphase with $H_{\rm ac}$ resulting in *negative* local μ' and $B'_{\rm ac}$. Such a negative $B'_{\rm ac}$ is in striking contrast to all the common ac susceptibility models [11–19] that predict a positive $B'_{\rm ac}$ everywhere in the bulk of the sample. The main source of the discrepancy is that in the standard models vortices penetrate and leave the sample during the cycle of the ac field. In our case, however, the GB enforces an invariant number of vortices inside the sample. Therefore the vortex droplet undergoes only compressional deformations that result in positive μ' in the center and negative μ' closer to the edges. Note that the global μ' of the entire sample is always positive, and such a unique negative response can be observed only by use of local measurements.

Figures 3(a) and 4 show, respectively, the calculated and experimental $B'_{\rm ac}$ at $T = 77.5$ K as a function of $H_{\rm dc}$ at several locations. At $x = 0$ a positive $B'_{\rm ac}$ appears with the formation of the vortex droplet at $H_{\rm dc} = H_p - H_{\rm ac}$. Away from the center, however, $B'_{\rm ac} = 0$ as long as

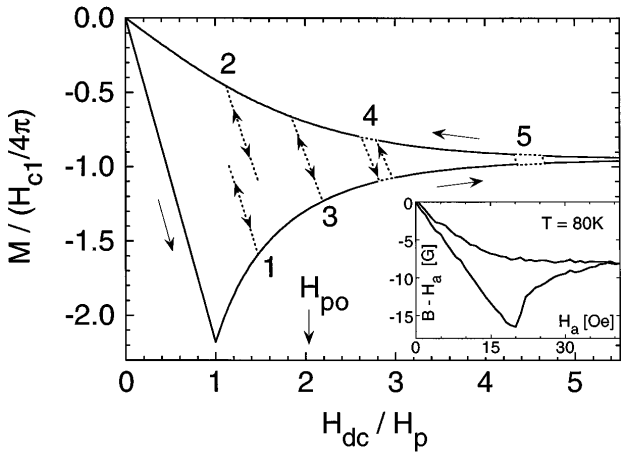

FIG. 2. The theoretical global dc magnetization loop (solid) and several ac trajectories (dashed) due to geometrical barrier ($d/W = 0.2$, $H_{\rm ac} = 0.17H_p$). Maximum ac dissipation occurs at point 4. Inset: experimental local magnetization loop $B_{\rm dc} - H_{\rm dc}$ in the central region of BSCCO crystal at $T = 80$ K.

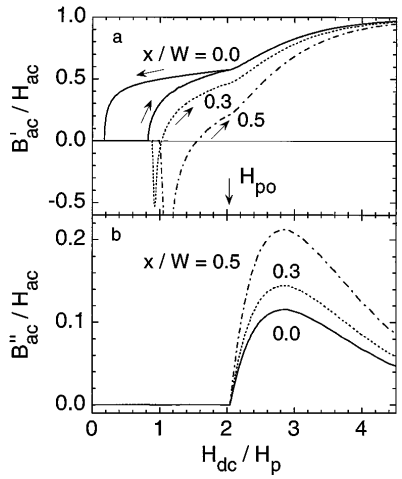

FIG. 3. Calculated (a) $B'_{\rm ac}$ and (b) $B''_{\rm ac}$ at three locations as a function of $H_{\rm dc}$. Negative $B'_{\rm ac}$ appears in the vicinity of H_p for $x/W > 0$. The dissipation sets in at $H_{\rm po}$ accompanied by a kink in $B'_{\rm ac}$. $B'_{\rm ac}$ is hysteretic at $H_{\rm dc} < H_{\rm po}$ (shown only for $x = 0$). $B'_{\rm ac}$ is largest at $x = 0$ and $B''_{\rm ac}$ is largest close to the edges.

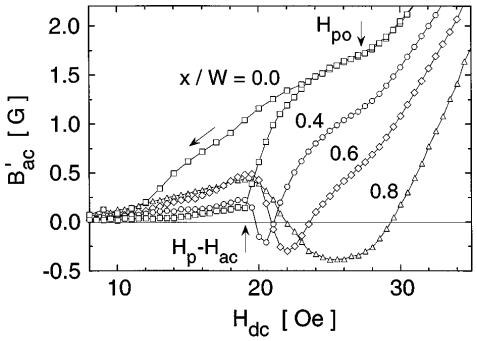

FIG. 4. B'_{ac} at four locations across BSCCO crystal as a function of increasing H_{dc} showing the negative B'_{ac} above the penetration field. The hysteretic behavior below H_{po} is shown at $x = 0$. $T = 77.5$ K, $H_{ac} = 5$ G rms, and $f = 37$ Hz.

the size of the droplet is small. As H_{dc} increases the droplet edge b reaches the observation point x, resulting in negative B'_{ac} that gradually turns positive with the further increase of H_{dc}. The negative B'_{ac} occurs at progressively higher H_{dc} at larger x/W. Furthermore, Figs. 3(a), 4, and 5(a) clearly demonstrate that $B'_{ac}(x)$ has a *maximum* value at $x = 0$. This result is an additional significant contradiction to the standard models which predict *minimum* B'_{ac} (maximum screening) in the center [11–19]. Our model describes strictly a 2D sample that results in an infinite slope of $B_z(x)$ at the droplet edges in Fig. 1 and, hence, a very steep onset of negative B'_{ac} in Fig. 3(a). In reality $B_z(x)$ varies smoothly on the range on the order of the sample thickness resulting in a smooth B'_{ac} as observed in Fig. 4. The small positive upturn of B'_{ac} at $H_{dc} < H_p$ is an artifact due to finite separation between the sample and active layer of the sensors.

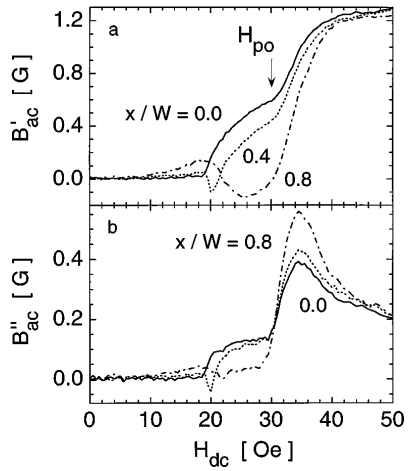

FIG. 5. (a) B'_{ac} and (b) B''_{ac} on increasing H_{dc} at $T = 80$ K, $H_{ac} = 1.5$ G rms, and $f = 37$ Hz at three locations. The dissipation peak due to the collapse of geometrical barrier sets in at H_{po}. The finite B''_{ac} below H_{po} is due to small viscous dissipation within the vortex droplet.

Another interesting observation is the hysteresis in local B'_{ac} as a function of H_{dc} at low fields as shown in Figs. 3(a) and 4. This hysteresis is another characteristic feature of the GB that is not obtained in other models. On the decreasing branch of the dc magnetization loop the vortex droplet extends to the sample edges [20,24]. The deformation of the dome by H_{ac} results in negative B'_{ac} only close to the sample edges, whereas the rest of the sample displays a positive B'_{ac} that is larger on decreasing H_{dc} than on increasing field. This local hysteresis is clearly shown both theoretically and experimentally in Figs. 3(a) and 4, respectively (presented only for $x = 0$ for clarity). Note that in global measurements, on the other hand, the total χ' displays almost no hysteresis since trajectories 1 and 2 in Fig. 2 have very similar slopes.

We now turn to the discussion of the dissipation peak. At low H_{dc} the ac trajectories such as 1 and 2 in Fig. 2 are fully reversible with no dissipation, and $B''_{ac} = 0$ as shown in Fig. 3(b). In fact, the displacement of vortices inside the droplet (Fig. 1) and within the edge region should cause some dissipation due to finite vortex viscosity as observed experimentally in Fig. 5(b) ($T = 80$ K) by finite values of B''_{ac} at $H_{dc} < H_{po}$. This dissipation may become significant at high frequencies, but it is small at lower frequencies, and is ignored in our calculations. As H_{dc} increases, the width of the dc magnetization loop decreases, and at some point the amplitude of H_{ac} becomes sufficient to bridge between the ascending and descending branches of the dc loop as shown by trajectory 3 in Fig. 2. We denote the dc field at this point as the pinch-off field H_{po}. At $H_{dc} > H_{po}$ the ac magnetization trajectory becomes hysteretic, and as a result dissipation sets in. The dissipation is proportional to the area encircled by the ac trajectory which reaches a sharp maximum at point 4. At higher field the dissipation decreases again as the magnetization loop shrinks (point 5). The corresponding theoretical and experimental behaviors of the local B_{ac} in Figs. 3 and 5 show a remarkable agreement, especially in view of the simplicity of the theoretical model. Three distinct features are predicted at H_{po}: sharp onset of B''_{ac}, kink in B'_{ac}, and hysteretic B'_{ac} at $H_{dc} < H_{po}$. All these features are clearly resolved experimentally in Figs. 4 and 5. Also, as mentioned above, the experimental $B'_{ac}(x)$ is largest at $x = 0$, and $B''_{ac}(x)$ is highest close to the edges in accord with the model. In addition, the dissipation peaks are asymmetric with a slower falloff at the high-field side. An important conclusion of these results concerns the origin of the dissipation peak. This peak is normally attributed to bulk vortex properties such as the onset of critical current, phase transition in vortex pinning mechanism, or a sharp decrease in flux flow or flux creep resistivity [14–19]. In contrast, our analysis of the ac response [Eqs. (1)–(3)] does not include any parameters related to these vortex properties, and therefore the observed dissipation peak in BSCCO crystals at elevated temperatures is

completely *unrelated* to the resistivity behavior [23]. The peak is due entirely to GB. At $H_{dc} < H_{po}$ the GB screens H_{ac} very efficiently, and the number of vortices in the bulk is constant. At $H_{dc} > H_{po}$ the barrier "collapses," and vortices enter and exit the sample irreversibly during the ac cycle. Vortices enter at high potential energy and exit at a lower potential, resulting in energy dissipation due to work carried out by the external field. This dissipation is independent of the flux flow resistivity and is governed only by the properties of the GB.

Several additional significant features to be noted are the following: (i) At $H_{dc} > H_{po}$ the hysteretic ac trajectories result in anharmonic χ, causing a sharp onset of higher harmonics in the ac response. This nonlinear behavior is again the result of GB and does not reflect any change in bulk vortex properties [3,9]. (ii) The position of H_{po} and of the dissipation peak is sensitive to the amplitude of the ac field, and it shifts to lower fields with increasing ac amplitude. (iii) The above description can be readily applied to the temperature dependence of the ac response by introducing $H_{c1}(T)$ in Eqs. (1)–(3) with $B_{ac}(T)$ behaving similarly to the described $B_{ac}(H_{dc})$. (iv) Our treatment applies also to the case of Bean-Livingston surface barriers [28] in platelet geometry in which case H_{c1} has to be replaced by a characteristic field H_s. The surface barrier was pointed out as a source of ac losses and irreversibility previously [10,13,23,27,29]. The main difference between the two barriers is that a strong thermal relaxation over the surface barrier is expected [30] that results in a frequency dependent ac response. In pure GB the response is frequency independent. (v) Finally, at lower temperatures ($T \lesssim 40$ K) significant bulk pinning in BSCCO crystals is present [31] which requires the advance of a more general analysis that combines the bulk and surface effects in flat geometries.

In conclusion, the local ac response in the presence of geometrical and surface barriers has very distinct features that are not readily resolved by global susceptibility measurements. In clean BSCCO crystals at elevated temperatures, B'_{ac} has a maximum value in the center of the sample and may attain negative values closer to the edges, in contrast to the critical state and the flux-creep or flux-flow models. The dissipation peak and the onset of higher harmonics at characteristic field or temperature indicate the collapse of the barrier rather than a phase transition or a change in the bulk vortex properties.

We thank H. Motohira for providing the BSCCO crystals and H. Shtrikman for growing the GaAs heterostructures. Discussions with M. Konczykowski, C. J. van der Beek, and John R. Clem are gratefully acknowledged. This work was supported by the German-Israeli Foundation for Scientific Research and Development-GIF, and by the Israeli Ministry of Science and the Arts and the French Ministry of Research and Technology-AFIRST.

[1] A. P. Malozemoff *et al.,* Phys. Rev. B **38**, 7203 (1988).
[2] P. L. Gammel *et al.,* Phys. Rev. Lett. **61**, 1666 (1988).
[3] A. Shaulov and D. Dorman, Appl. Phys. Lett. **53**, 2680 (1988).
[4] L. Krusin-Elbaum *et al.,* Phys. Rev. Lett. **67**, 3156 (1991).
[5] A. Gupta *et al.,* Phys. Rev. Lett. **63**, 1869 (1989).
[6] M. Ziese *et al.,* Supercond. Sci. Technol. **7**, 869 (1994).
[7] J. Gilchrist and M. Konczykowski, Physica (Amsterdam) **212C**, 43 (1993).
[8] H. Pastoriza *et al.,* Phys. Rev. Lett. **72**, 2951 (1994).
[9] Y. Wolfus *et al.,* Physica (Amsterdam) **224C**, 213 (1994).
[10] C. J. van der Beek *et al.,* Phys. Rev. B **51**, 15 492 (1995).
[11] C. P. Bean, Rev. Mod. Phys. **36**, 31 (1964).
[12] A. M. Campbell, J. Phys. C **4**, 3186 (1971).
[13] J. R. Clem, J. Appl. Phys. **50**, 3518 (1979).
[14] E. H. Brandt, Phys. Rev. Lett. **67**, 2219 (1991); **68**, 3769 (1992); **71**, 2821 (1993); Phys. Rev. B **49**, 9024 (1994).
[15] V. B. Geshkenbein *et al.,* Phys. Rev. B **43**, 3748 (1991).
[16] C. J. van der Beek *et al.,* Phys. Rev. B **48**, 3393 (1993).
[17] M. A. Skvortsov and V. B. Geshkenbein, Zh. Eksp. Teor. Fiz. **105**, 1379 (1994) [Sov. Phys. JETP **78**, 743 (1994)].
[18] J. R. Clem and A. Sanchez, Phys. Rev. B **50**, 9355 (1994).
[19] R. Prozorov, A. Shaulov, Y. Wolfus, and Y. Yeshurun, J. Appl. Phys. **76**, 7621 (1994); Phys. Rev. B **52**, 12 541 (1995).
[20] E. Zeldov *et al.,* Phys. Rev. Lett. **73**, 1428 (1994); Physica (Amsterdam) **235C–240C**, 2761 (1994).
[21] Th. Schuster *et al.,* Phys. Rev. Lett. **73**, 1424 (1994).
[22] M. V. Indenbom *et al.,* Physica (Amsterdam) **235C–240C**, 201 (1994).
[23] C. J. van der Beek, Z. Sungaila, and G. Crabtree, Bull. Am. Phys. Soc. **40**, 791 (1995).
[24] M. Benkraouda and J. R. Clem (to be published).
[25] M. Marchevsky *et al.,* Phys. Rev. Lett. **75**, 2400 (1995).
[26] E. Zeldov *et al.,* Nature (London) **375**, 373 (1995).
[27] D. Majer *et al.,* Phys. Rev. Lett. **75**, 1166 (1995).
[28] C. P. Bean and J. D. Livingston, Phys. Rev. Lett. **12**, 14 (1964).
[29] M. Konczykowski *et al.,* Physica (Amsterdam) **194C**, 155 (1992); M. Konczykowski, *Progress in High Temperature Superconductivity* (World Scientific, Singapore, 1992), Vol. 30, p.152.
[30] L. Burlachkov *et al.,* Phys. Rev. B **50**, 16 770 (1994).
[31] E. Zeldov *et al.,* Europhys. Lett. **30**, 367 (1995).